

Article

Bioleaching of Zinc from Blast Furnace Cast House Dust

Amaia Sasiain ^{1,*} , Sophie Thallner ¹, Clemens Habermaier ¹, Sabine Spiess ¹ , Ludwig Birklbauer ², Martin Wallner ² and Marianne Haberbauer ¹

¹ K1-MET GmbH, Stahlstrasse 14, 4020 Linz, Austria

² Voestalpine Stahl GmbH, voestalpine-Strasse 3, 4020 Linz, Austria

* Correspondence: amaia.sasiain@k1-met.com

Abstract: Metallurgical dusts are by-products from steel manufacturing. The high iron content of cast house dust (~64%) makes this by-product an interesting iron feedstock alternative. Therefore, its return into the internal steelmaking circuit, specifically in the sinter plant, is a common practice in the steel industry. However, this dust fraction also contains heavy metals, as zinc. As a result of the re-entry of zinc into the process, the zinc concentration in the blast furnace flue gas dust also increases. This prevents the full recirculation of the blast furnace flue gas dust in the steelmaking process despite its relatively high iron content (~35%), thus causing part of the blast furnace flue gas dust to end in the landfill. The goal of this study was to investigate the usage of bacteria, such as the sulfur oxidizing *Acidithiobacillus thiooxidans* or the iron and sulfur oxidizing *Acidithiobacillus ferrooxidans*, to leach the undesirable element zinc from the cast house dust while preventing the leaching of iron, by adjusting the sulfur addition and avoiding, at the same time, the accumulation of sulfur in the solid fraction. Experiments proved that a co-culture of *A. thiooxidans* and *A. ferrooxidans* can effectively leach zinc from metallurgical dusts, maintaining high iron concentrations in the material. The influence of elemental sulfur on the efficiencies reached was shown, since higher removal efficiencies were achieved with increasing sulfur concentrations. Maximum zinc leaching efficiencies of ~63% (*w/w*) and an iron enrichment of ~7% (*w/w*) in the remaining residue were achieved with sulfur concentrations of 15 g/L for cast house gas concentrations of 125 g/L.

Keywords: blast furnace cast house dust; zinc removal; *Acidithiobacillus ferrooxidans*; *Acidithiobacillus thiooxidans*; bioleaching; metallurgical dust recycling; circular economy



Citation: Sasiain, A.; Thallner, S.; Habermaier, C.; Spiess, S.; Birklbauer, L.; Wallner, M.; Haberbauer, M. Bioleaching of Zinc from Blast Furnace Cast House Dust. *Minerals* **2023**, *13*, 1007. <https://doi.org/10.3390/min13081007>

Academic Editor: Chiharu Tokoro

Received: 16 June 2023

Revised: 20 July 2023

Accepted: 26 July 2023

Published: 28 July 2023



Copyright: © 2023 by the authors. Licensee MDPI, Basel, Switzerland. This article is an open access article distributed under the terms and conditions of the Creative Commons Attribution (CC BY) license (<https://creativecommons.org/licenses/by/4.0/>).

1. Introduction

The solid and sludge by-products generated during steel production represent a source of secondary resources due to their considerable content of valuable materials. The usage of technologies for the valorization of residues could, therefore, lower the demand for raw materials while reducing landfilling, resulting in economic savings for the steel industry and closing material cycles [1]. Despite the existence of several methods for the recovery of metals from metallurgical subproducts [2–4], limited literature references where bioleaching processes were used as a metal recovery technique from steel mill by-products were found [5–8]. The current study is, to our knowledge, the first to focus on the cast house dust treatment through the utilization of extremely acidophilic bacteria to remove the element zinc, while preventing the leaching of iron. For this reason, the leaching efficiency, as well as the influence of the sulfur in the leaching process, together with the composition of the solid cast house gas dust, were also investigated during this study.

Zinc is naturally present in iron ores (loaded into the blast furnace in the form of ferrites, silicates, or sulfides), as well as in the recycled materials. The zinc compounds which enter the blast furnace react with the reducing gas at temperatures exceeding the boiling point of zinc, forming metallic zinc vapor which ascends with the gas to the colder parts of the blast furnace where it is re-oxidized again to form zinc oxide (ZnO). While

part of the condensed zinc phases leave the furnace together with the gas, the remaining amount descends, forming a cyclical pattern as illustrated in Figure 1 [9,10].

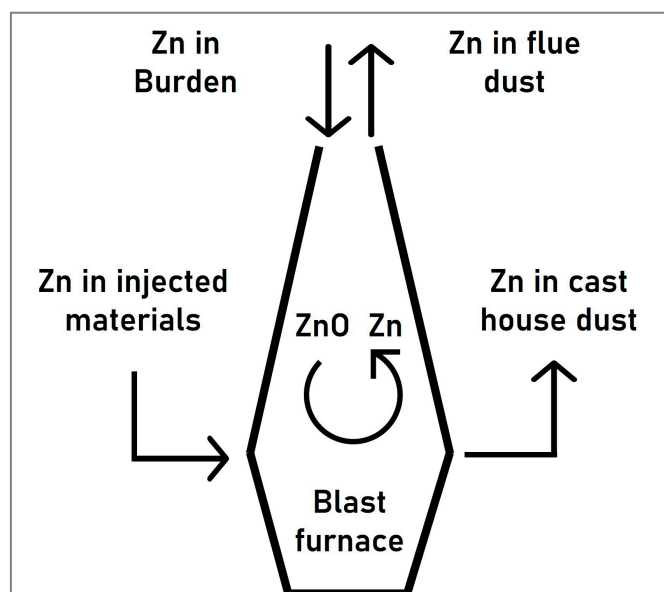


Figure 1. Cyclical behavior of zinc in the blast furnace.

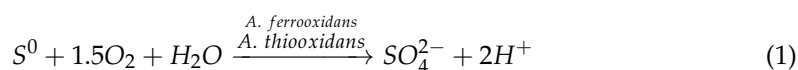
The accumulation of zinc in the blast furnace has some detrimental effects, such as the increase of the reductant rate and the reduction of the lining life of carbon-based brick materials or scaffold formation, which may lead to deteriorating the furnace performance [9,10]. Since the restriction of the zinc content in the blast furnace is mainly achieved by regulating the input levels of this element, a pre-separation of the zinc present in the by-products entering the blast furnace or upstream processes would be very interesting to avoid the abovementioned problems.

The by-product cast house dust, with an iron content of around 65% (w/w), is an interesting source of iron. Therefore, the removal of the zinc content for its further reutilization in the steel mill was analyzed during this research. The cast house dust is emitted into the cast house of a blast furnace as a consequence of the casting of liquid iron and slag [11]. Conventionally, around 2.8 kg of cast house dust are produced per ton of hot metal [12]. Since cast house dust is commonly recycled to the sinter process, elevated zinc concentrations in the cast house dust would make it difficult to fully recirculate blast furnace flue gas dust, as its recirculation will favor the zinc enrichment in the system. Consequently, part of the blast furnace flue gas dust ends up in landfills. Therefore, separation of the zinc present in the cast house dust would enhance the recycling rates of the blast furnace dust.

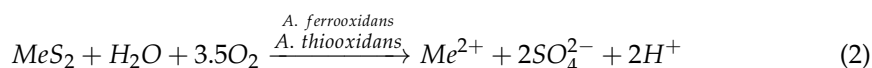
The current processes focused on the recovery of metals from steel mill dust can be classified into the following categories: physical, hydrometallurgical, and pyrometallurgical processes [2]. As acid leaching occurs at low pH (1.5–2), traditionally, it represents the predominant method for the removal of metals from wastes. However, other methods such as microbial leaching have emerged in recent years for the removal of heavy metals such as zinc [13], since it is environmentally friendlier, has lower energy necessities, and fewer chemical-associated costs when compared to chemical leaching [14]. The usage of microbial processes in metal extraction is usually known as bioleaching [13]. The microorganisms commonly used for bioleaching applications are extremely acidophilic ($\text{pH} < 3$) and mesophilic, which means that those organisms grow optimally in relatively acid environments and at moderate temperature. Bacterial leaching of metal oxides from solid materials is mainly facilitated by biogenic production of inorganic and organic acids and the secretion of complexing agents [15]. Some microorganisms, especially those which belong to the *Acidithiobacillus* genus, can improve the leaching of metal sulfides [13].

Acidithiobacillus ferrooxidans is an acidophilic bacterium which obtains energy from the oxidation of sulfide minerals (e.g., FeS₂, CuFeS₂), ferrous oxide (FeO), and elemental sulfur [13,15]. *A. ferrooxidans* converts insoluble metal sulfides or oxides into water soluble metal sulfates through biochemical oxidation reactions [16]. The optimal growth conditions for *A. ferrooxidans* are a pH between 2 and 2.5 and a temperature in the range of 28–35 °C [17]. *Acidithiobacillus thiooxidans* obtains energy derived from the oxidation of elemental sulfur and reduced inorganic sulfur compounds to support its autotrophic growth. *A. thiooxidans* grows in the optimum pH range of 2.0–3.5, being the optimum temperature 28–30 °C [18]. The mechanisms proposed for biological metal leaching are the following:

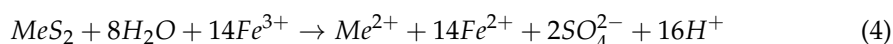
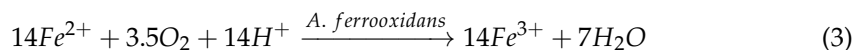
- In the first mechanism, *A. ferrooxidans* and *A. thiooxidans* produce sulfuric acid according to Equation (1) [15]. This sulfuric acid is responsible for the dissolution of the waste matrix surrounding the metal sulfides or oxides and facilitates the production of soluble metal sulfates [19].



- In the second mechanism, shown in Equation (2), *A. ferrooxidans* interacts with the insoluble metal sulfides (MeS) causing the release of the metal, which is a free metal ion (Me²⁺). The microorganisms adhere to the surface of sulfide mineral and solubilize the metal directly [20].



- In the third mechanism, *A. ferrooxidans* oxidizes Fe²⁺ to form Fe³⁺, as presented in Equation (3). The oxidation of Fe²⁺ to form Fe³⁺ by iron-oxidizing bacteria leads to the dissolution of acid-soluble and acid non-soluble metal sulfides [19], since Fe³⁺ subsequently causes the chemical leaching of metal-bearing minerals, as seen in Equation (4), which is a purely chemical process [20].



In this study, elemental sulfur (S⁰) was added, since it acts as a substrate for the production of sulfuric acid (Equation (1)). During the sulfur dosage, care was taken not to exceed the amount of sulfur needed for the microorganisms to avoid the accumulation of sulfur in the cast house dust, as the solid residue, once zinc is reduced, is going to be reinjected in the steel mill.

2. Materials and Methods

2.1. Materials and Chemicals

The cast house dust composition was analyzed, with iron resulting as the main component at ~64% (w/w) and zinc at ~3% (w/w), respectively. Other elements as aluminum, lead, chromium, or sulfur were also detected, being the sum of the overall concentrations lower than 0.6% (w/w).

All chemicals were of analytical grade, purchased from Sigma-Aldrich (St. Louis, MI, USA) and all solutions were prepared using deionized water.

2.2. Bacterial Strain and Medium

Cultivation of the microbial population was performed in a sulfur medium, according to Wakeman et al. [21]. The composition of the growth medium contained (mg/L) Na₂SO₄·10H₂O (150), (NH₄)₂SO₄ (450), KCl (50), MgSO₄·7H₂O (500), KH₂PO₄ (50), Ca (NO₃)₂·4H₂O (14), and 5, 7.5, or 15 (g/L) of sulfur powder. Those components (except the sulfur) were dissolved in deionized water and sterilized for 20 min at 121 °C. The pre-cultivation phase was performed at 30 °C and 160 rpm, using a co-culture of *A. thioox-*

idans (DSM No. 504) and *A. ferrooxidans* (DSM No. 583). The bacteria were purchased from DSMZ.

2.3. Stirred Tank Reactor Setup

A double jacketed continuous stirred tank reactor (CSTR) (Schmizo AG, Oftringen, Switzerland), with a working volume of 3 L, was used for the experiments. The temperature, pH, and redox potential were continuously monitored with an AwiComb automated control unit (Awite Bioenergy GmbH, Langenbach, Germany). Two electrodes (Mettler Toledo GmbH, Vienna, Austria) were used to measure the redox potential and the pH. The reactor was heated to 30 °C using a water bath (Proline P 8, LAUDA, Regau, Austria) and the solution was mixed with the help of a motor-stirrer set up to 160 rpm. Aeration of the system was achieved using an air pump (Schege M2K3, SCHEGO Schemel & Goetz GmbH & Co KG, Offenbach, Germany) which was set to 75 L/h, measured by a rotameter. A schematic representation of the stirred tank system can be seen in Figure 2.

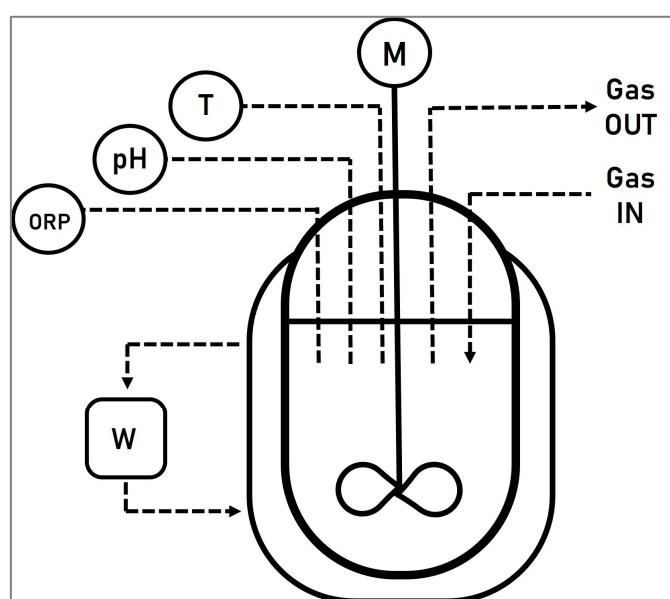


Figure 2. Schematic representation of the stirred tank system, where ORP symbolizes the redox electrode to measure the oxidation reduction potential, pH represents the pH electrode, T illustrates the temperature electrode, and, finally, W and M represent the water bath and the motor, respectively.

2.4. Methodology

Prior to each bioleaching experiment, the CSTR, containing the growth medium, was inoculated with a co-culture of *A. ferrooxidans* and *A. thiooxidans* (10% (v/v)), and was pre-cultivated for one week at 30 °C, 160 rpm, and 75 L/h air, adding the corresponding sulfur amount to each run. Three experiments with different sulfur concentrations and cast house dust concentrations were carried out (see Table 1). The goals of this experiments were: (I) the determination of the ideal sulfur concentration to cover the microorganisms' necessities and, therefore, produce the highest amount of sulfuric acid, and (II) the leaching of the highest achievable zinc share while obtaining the lowest possible remaining sulfur in the already treated solid residue.

Table 1. Experimental conditions.

Series	Sulfur [g/L]	Cast House Dust [g/L]
run1	5	50, 75, 100, 125
run2	7.5	50, 75, 100, 125
run3	15	50, 75, 100, 125

Since the exposure of the microorganisms to a residue could possibly affect the microorganisms [22], batch experiments were conducted with (10, 30, 40 and 50 g/L) in 250 mL shaker flasks prior to the CSTR tests. The results of these experiments showed that no inhibition occurred. Additionally, some literature sources show high Zn tolerance (up to 1071 mmol/L) of *Acidithiobacillus ferrooxidans* [23,24].

2.5. Bioleaching Experiments in CSTR

After a one-week pre-cultivation period, the evaporation losses were compensated with deionized water and, afterwards, the corresponding amount of cast house dust and elemental sulfur was added (as indicated in Table 1). To measure the concentration of the metals dissolved in the lixiviant, a liquid sample of the leachate was taken at the beginning (zero), middle (1 week), and end (2 weeks) of each cycle. Prior to elemental analyses, these samples were filtered through a 0.2 μm Chromafil filter (Macherey-Nagel, Düren, Germany). At the end of each cycle (2 weeks), a sample of the undissolved solid in the leachate was taken as well. The solid sample was filtered (through a 0.2 μm filter) and rinsed with deionized water until the pH of the permeate was close to neutral to prevent further oxidation reactions. The pH of the leachate was analyzed with a pH meter (Knick pH Meter 765, Berlin, Germany) and the microorganism population from the leachate was qualitatively quantified using a Carl Zeiss microscope (Axio Lab A1, Jena, Germany).

The first run started with 50 g/L cast house dust and 5 g/L sulfur. Increasing amounts of dust were added every 2 weeks as specified in Table 1, in order to study the behavior of the leaching efficiency with increasing amounts of dust. However, the addition of this material was not arbitrary. To start a new stage, two thirds of the stirred tank content had to be pumped out and replaced with 2 L of sterile growth medium with its corresponding amount of sulfur (5, 7.5, or 15 g/L, for the runs 1, 2, and 3, respectively). The process was performed in this manner to maintain, in the reactor, a part of the microbial population which was already adapted to lower dust concentrations. The required amount of dust was added to an aliquot and the dust concentration was increased in the following steps: 50-, 75-, 100-, and 125 g/L.

2.6. Chemical and Crystallographic Analysis

The chemical composition of the samples was determined as follows: sulfur was analyzed according to DIN EN ISO 15350 (Leco CS-744). To measure chromium, zinc, and lead, the sample was decomposed in a high-pressure autoclave (Ultraclave MLS) with a mixture of nitric and hydrofluoric acid. Afterwards, the decomposed liquid samples were analyzed using ICP-OES (Spectro Arcos) or ICP-MS (Thermo Scientific iCAP RQ, Waltham, MA, USA) for Cr and Zn and Pb, respectively. For iron and aluminium determination, the sample was decomposed in a mixture of hydrochloric and perchloric acid according to OENORM EN ISO 439, and afterwards measured with ICP-OES.

X-ray diffraction analysis (XRD) was implemented for the crystallographic analysis. The XRD analyses were performed using a Panalytical X'Pert PRO MPD diffractometer with Bragg-Brentano geometry and Cobalt $K\alpha_1$ radiation with a wavelength of 1.789010 Å at 35 kV and 40 mA. A 1-D RTMS detector (X'Celerator) and a $K\beta$ (Fe)-filter were also used to achieve high sensitivity and noise reduction. The sample preparation was conducted manually using a mortar to achieve a fine pulverization, thereby reducing the effects of any preferred orientation and obtaining a better signal due to smaller particle sizes.

The measurements were performed with a step size of $0.0167^\circ 2\theta$ and the angular range extended from $15\text{--}130^\circ 2\theta$. The total measurement time per sample was three hours and four minutes, during which the samples were continuously rotated to achieve better statistical accuracy of the measurements. The collected data were processed using Panalytical HighScore Plus 3.0.5 software. Quantitative phase analyses were performed using the Rietveld method.

2.7. Calculation of the Leaching Efficiency and Metal Removal Efficiency

The leaching efficiency (L_{eff}) from the leachate collected was calculated as follows:

$$L_{eff}[\%] = \frac{(C_A \times V_T) - (C_{PS} \times V_R)}{(C_D \times M_D)} \times 100$$

where C_A is the actual measured metal concentration in [mg/L], V_T is the total volume of the reactor in [L], C_{PS} is the final metal concentration of the previous stage measured in [mg/L], V_R is the rest volume of the previous stage which remains in the reactor in [L], C_D is the initial metal concentration in the untreated dust in [mg/kg], and M_D is the dust mass used in the present stage in [kg].

The metal removal efficiency of the solid samples was calculated as follows:

$$M[\%] = \frac{\left(\left(\frac{W_A \times M_T}{100} \right) - \left(\frac{M_A \times W_i}{100} + (M_T - M_A) \times \frac{W_B}{100} \right) \right) \times 100}{\left(\frac{M_A \times W_i}{100} + (M_T - M_A) \times \frac{W_B}{100} \right)} \quad (5)$$

where M is the mass loss or mass increase in [%], W_A is the actual measured metal concentration in [%], M_T is the total dust mass (dry) present in the reactor in the present stage in [g], M_A is the fresh dust mass added in the present stage (dry) in [g], W_i is the measured metal concentration in the untreated dust in [%], and W_B is the metal concentration measured in the previous stage in [%]. The remaining sulfur content (S) in the solid samples was additionally calculated as follows (Equation (6)).

$$S[g] = S_f - S_i = \left(\frac{M_T \times W_{SA}}{100} \right) - \left(\frac{M_A \times W_S}{100} + \frac{(M_T - M_A) \times W_{SB}}{100} \right) \quad (6)$$

where S_f is the final sulfur amount in [g] present in the reactor in the present stage after 2 weeks of experiments, S_i is the initial sulfur in [g] in the reactor in the present stage initially, right after the addition of fresh sulfur and dust, W_{SA} is the measured sulfur concentration in the present stage in [%], M_T is the total dust mass (dry) present in the reactor in the present stage in [g], M_A is the fresh dust mass added in the present stage (dry) in [g], W_S is the measured sulfur concentration in the untreated dust in [%], and W_{SB} is the sulfur concentration measured in the previous stage in [%].

3. Results and Discussion

3.1. Cast House Dust Characterization

The chemical, as well as the crystallographic, structure of the cast house dust was analyzed. The results of the chemical analysis reflected the predominance of iron and zinc in the cast house gas with 64.4% (w/w) and 2.9% (w/w), respectively (Table 2), with the sum of the rest of the elements (Al, Pb, Cr and S) amounting to less than 1% (w/w). On the other hand, the XRD analysis showed that the cast house dust is mainly composed by magnetite, hematite and zinc bounded as oxide and sulfate (Figure 3).

Table 2. Selected element content of cast house dust.

Compound	Al	Pb	Cr	Fe	S	Zn
[% (w/w)]	0.170	0.010	0.008	64.350	0.404	2.870

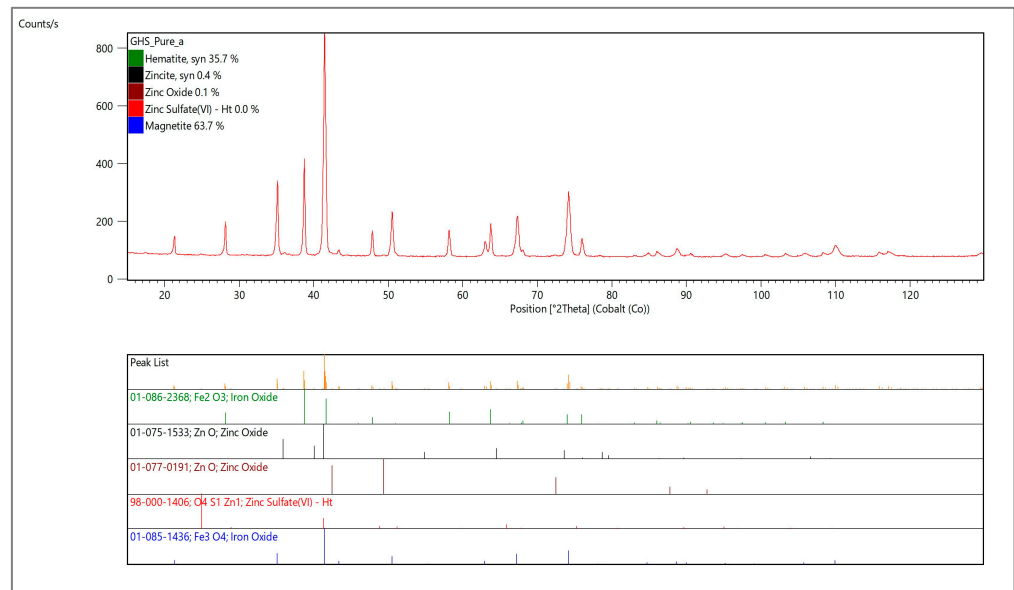


Figure 3. X-ray diffractogram to analyze the crystallographic structure of the untreated cast house dust.

3.2. run1: Addition of 5 g/L Sulfur

Figure 4 shows the leaching efficiencies for the selected metals (Fe, Zn, as well as Al, Pb, Cr). Whereas the leaching efficiency for Al exhibits a nearly constant behavior (17%) through the whole dust concentrations range, the leaching efficiencies for Fe, Zn, Cr, and Pb present a decrease with increasing cast house dust concentrations, reaching leaching efficiencies of 3%, 40%, 9%, and 0%, respectively, for 125 g/L of cast house dust. Despite the pH increasing with growing cast house dust amounts, it remained very low, even for the highest cast house dust concentrations (125 g/L).

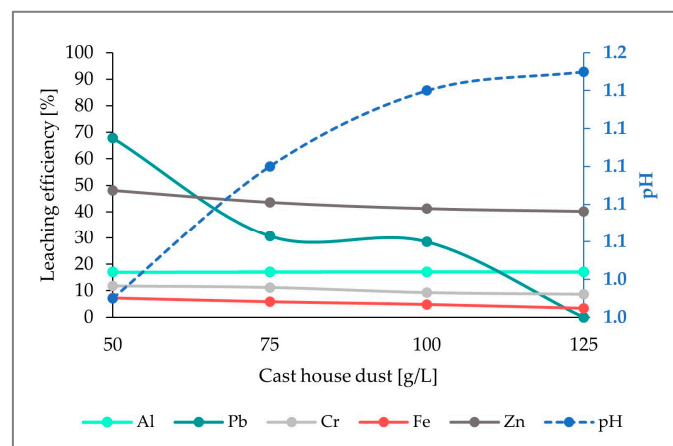


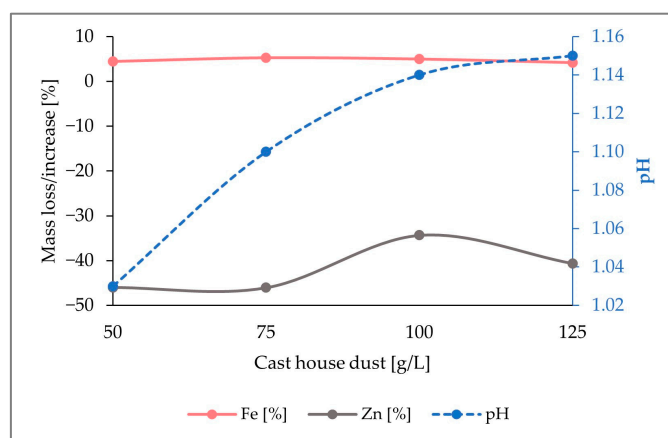
Figure 4. Leaching efficiency for Al, Pb, Cr, Fe, and Zn, as well as the pH for an addition of 5 g/L of sulfur and increasing cast house gas concentrations.

Table 3 shows the iron enrichment in the solid samples for different dust concentrations and 5 g/L sulfur. Around 10 g of iron were gained with a concentration of 125 g/L of dust. On the other hand, approximately 4 g of zinc were removed from the solid dust sample at a loading rate of 125 g/L of cast house dust. Nevertheless, when focusing on the behavior of Al, Pb, or Cr, no significant mass increase or decrease was observed due to their very low concentrations in the dust.

Table 3. Al, Pb, Cr, Fe, and Zn mass fluctuations in the solid samples following addition of 5 g/L sulfur.

Cast House Dust [g/L]	Al Δm [g]	Pb Δm [g]	Cr Δm [g]	Fe Δm [g]	Zn Δm [g]
50	−0.03	−0.01	0.002	4.33	−1.90
75	−0.08	−0.01	0.006	7.70	−2.79
100	−0.14	−0.01	0.009	9.75	−2.72
125	−0.09	0.01	0.012	10.11	−4.02

In Figure 5, it is observed that, while up to 40% (*w/w*) of the zinc content present in the reactor was removed, about 4% (*w/w*) iron enrichment was achieved for dust concentrations of 125 g/L. Although a pH increase was noticed with rising cast house concentrations, the maximum level reached was below a pH of 1.2, which is far away from a critical pH range where the bacterial activity might get inhibited.

**Figure 5.** Fluctuation of the Fe and Zn mass share in the solid samples together with the evolution of the pH by the addition of 5 g/L sulfur with increasing concentrations of cast house dust.

3.3. run2: Addition of 7.5 g/L Sulfur

In Figure 6, the calculated leaching efficiencies for Al, Pb, Cr, Fe, and Zn when adding 7.5 g/L sulfur are illustrated. Similarly to what happened when using 5 g/L of sulfur, the leaching efficiency of Al presented a constant behavior (18%) along the entire experimental range, and diminishing leaching efficiencies were detected for the rest of the elements. Additionally, leaching efficiencies for the element Pb remained unchanged independently of the concentration of sulfur (68% and 0% for 50 g/L and 125 g/L, respectively, of cast house dust).

On the other hand, it was noticed that for run2, where 7.5 g/L of sulfur was used, the leaching efficiency of Fe, Zn, and Cr was slightly higher than that from run1, since the efficiencies reached for Fe, Zn, and Cr for a cast house dust concentration of 125 g/L were: 6%, 48%, and 11% compared to the 3%, 40%, and 9% obtained for 5 g/L. An analogous pH behavior to that observed in run1 was observed here. Growing cast house dust concentrations were linked to an increase in pH. However, the pH remained very low, even for 125 g/L cast house dust.

Table 4 shows a stepwise iron increase in the solid phase, achieving an enrichment of nearly 12 g for cast house dust concentrations under a loading rate of 100 g/L. Nevertheless, for higher dust concentrations (125 g/L), a severe drop in the iron enrichment was observed, going down to approximately 5 g. On the other hand, a progressive zinc removal with increasing dust concentrations was noticed, reaching a zinc removal of up to 4 g for 100 g/L dust. As observed in the prior experiment with 5 g/L of sulfur, no significant mass

oscillations for the elements Al, Pb, and Cr were observed, which might be caused by the scarce concentrations of those elements in the cast house dust.

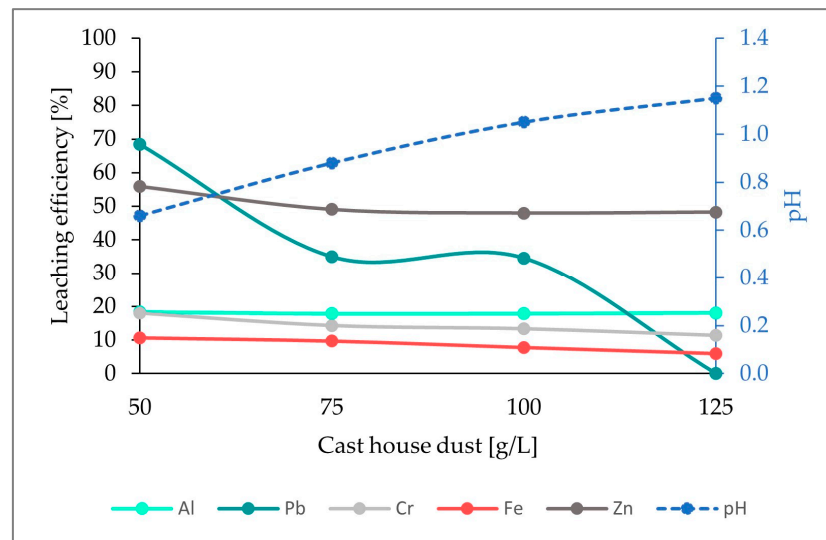


Figure 6. Leaching efficiency for Al, Pb, Cr, Fe and Zn as well as the pH for an addition of 7.5 g/L of sulfur for cast house dust concentrations between 50 and 125 g/L.

Table 4. Al, Pb, Cr, Fe, and Zn mass fluctuations in the solid samples by the addition of 7.5 g/L sulfur.

Cast House Dust [g/L]	Al Δm [g]	Pb Δm [g]	Cr Δm [g]	Fe Δm [g]	Zn Δm [g]
50	−0.03	−0.01	0.002	4.57	−2.16
75	0.08	−0.01	0.006	6.07	−3.02
100	−0.13	−0.01	0.009	11.48	−3.83
125	−0.05	0.01	0.012	4.54	−3.94

The drop in the iron enrichment observed can be explained by the figure below (Figure 7). As it can be observed, for a dust concentration of 100 g/L, the iron content enrichment was approximately 6% (*w/w*), whereas 49% (*w/w*) of zinc was removed from the solid phase. However, for a dust concentration of 125 g/L, the iron enrichment decreased to 2% (*w/w*) because of the downturn of the zinc removal, which decreased from 49% (*w/w*) to 42% (*w/w*).

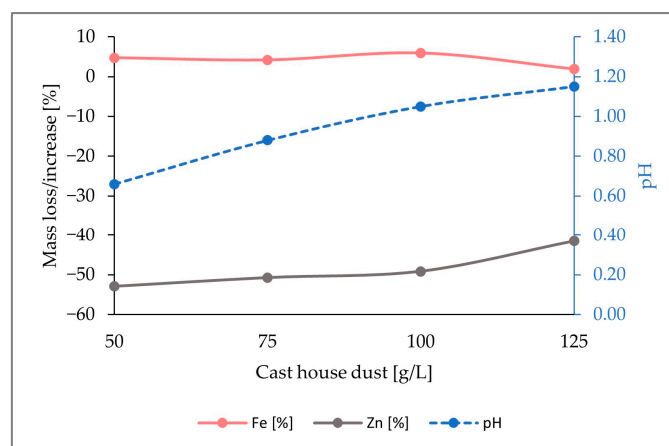


Figure 7. Representation of the mass share fluctuations for Fe and Zn, as well as pH change in the solid sample through the addition of 7.5 g/L sulfur, for growing cast house dust concentrations up to 125 g/L.

3.4. run3: Addition of 15 g/L Sulfur

As illustrated in the figure below (Figure 8), there is an obvious increase in the leaching efficiencies of all the elements analyzed when compared to the results from run1 and run2. Additionally, the leaching efficiencies achieved here are the highest efficiencies obtained compared to the experiments with 5 and 7.5 g/L of sulfur, achieving 14%, 63%, 23%, 28%, and 44% for Fe, Zn, Cr, Al, and Pb, respectively, and an addition of 125 g/L of cast house dust.

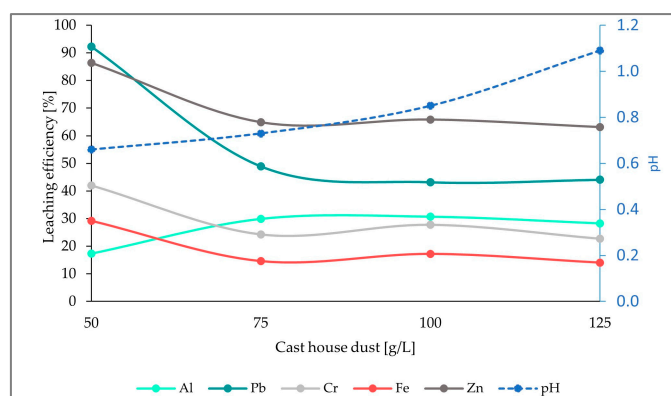


Figure 8. Leaching efficiency for Al, Pb, Cr, Fe, and Zn, as well as the pH for an addition of 15 g/L of sulfur and rising cast house dust concentrations.

Table 5 shows that increasing elemental sulfur concentrations are connected to higher iron enrichment in the solid residual phase and higher zinc leaching shares. With a concentration of 125 g/L, for example, the iron content of the solid sample was observed to increase to 16 g, with a corresponding zinc loss of 5.5 g. These are the highest values reached when compared to the experiments with 5 and 7.5 g/L sulfur concentrations (run1 and run2). The behavior of Al, Pb, and Cr was constant and no large fluctuations in their concentrations were observed.

Table 5. Al, Pb, Cr, Fe, and Zn mass fluctuations in the solid sample following the addition of 15 g/L sulfur.

Cast House Dust [g/L]	Al Δm [g]	Pb Δm [g]	Cr Δm [g]	Fe Δm [g]	Zn Δm [g]
50	0.00	0.43	−0.001	−1.47	−1.61
75	0.21	−0.05	0.006	12.65	−3.95
100	0.47	0.00	0.009	12.16	−4.43
125	0.41	0.00	0.011	16.34	−5.36

In conclusion, the largest zinc removal efficiencies were achieved with 15 g/L of sulfur, which was the highest sulfur concentration among the three runs performed. As seen in Figure 9, for cast house dust concentrations of 125 g/L, 58% (*w/w*) of the zinc present in the solid sample was leached. Therefore, it can be concluded that, for the same dust concentrations, higher sulfur-addition shares show larger zinc removal efficiencies, since a 58% (*w/w*) zinc removal efficiency was reached with 15 g/L of sulfur and 125 g/L of cast house dust, while only 41% (*w/w*) and 42% (*w/w*) were achieved for lower sulfur concentrations (5 g/L and 7.5 g/L, respectively) and 125 g/L of cast house dust.

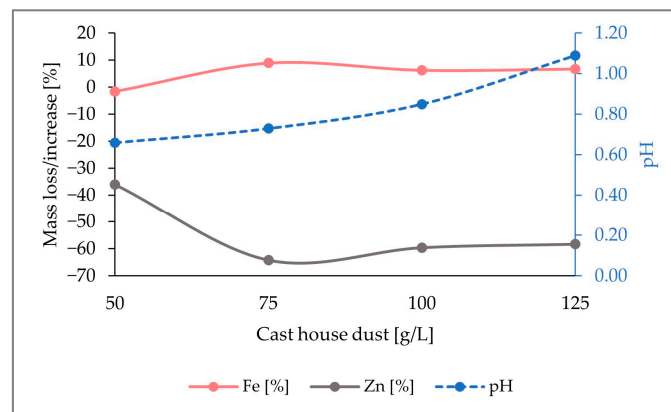


Figure 9. pH variation and percentage of mass loss or increase of Fe and Zn in the solid sample through the addition of 15 g/L sulfur for cast house dust concentrations between 50 and 125 g/L.

4. Influence of Sulfur Concentration on Bioleaching of Zinc and Iron

The leaching efficiencies for zinc for the three set of experiments with different sulfur and cast house dust concentrations were calculated and are presented in the figure below (Figure 10), concluding that higher leaching efficiencies can be achieved with higher sulfur concentrations.

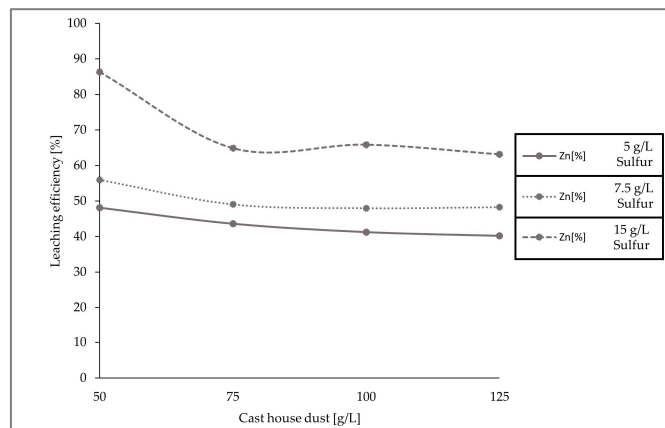


Figure 10. Leaching efficiencies of zinc with 5, 7.5, and 15 g/L sulfur concentrations and increasing cast house dust share.

Figure 11, which presents the removal behavior of zinc in the solid sample for the three runs conducted with different sulfur and cast house dust concentrations, exhibits identical results with respect to the leaching efficiencies, showing higher zinc removal with higher sulfur concentrations. For example, for a cast house dust concentration of 125 g/L, the zinc removal achieved for sulfur concentrations of 7.5 and 5 g/L was ≤ 4 g, while when using 15 g/L of sulfur approximately 5.5 g of zinc was removed from the dust.

When looking at the loss of zinc and the iron content enrichment in the solid sample (Figure 12), it can be observed that the highest zinc removal efficiencies were reached with 15 g/L of sulfur. With dust concentrations above 75 g/L, the average removal efficiency of zinc from the cast house dust is 60% (w/w) when using 15 g/L of sulfur, 47% (w/w) for sulfur concentrations of 7.5 g/L, and around 40% (w/w) for 5 g/L of sulfur. On the other hand, the highest iron enrichment with dust concentrations higher than 75 g/L was also linked to higher sulfur concentrations, reaching beyond 7% (w/w), on average, iron enrichment for sulfur concentrations of 15 g/L. While results from other studies with *A. ferrooxidans* and similar metal concentrations showed iron losses of 30% (w/w) [13], the present study found rather low or no iron leaching at all during the three runs, an

advantageous fact since iron loss is prevented, enhancing the further reintroduction of the treated dust in the steel mill.

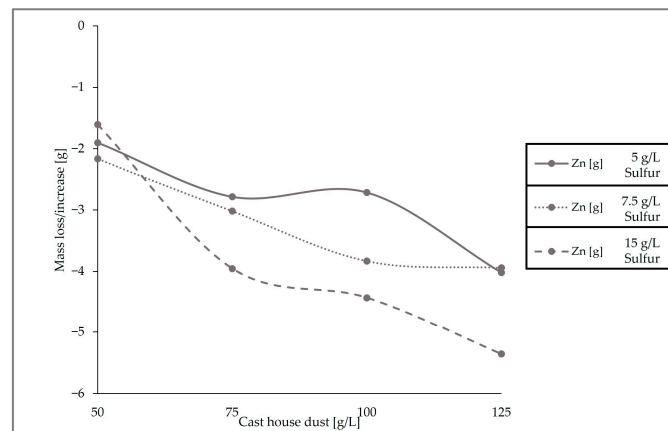


Figure 11. Zn mass deviation with different cast house dust concentrations for 5, 7.5, and 15 g/L of sulfur.

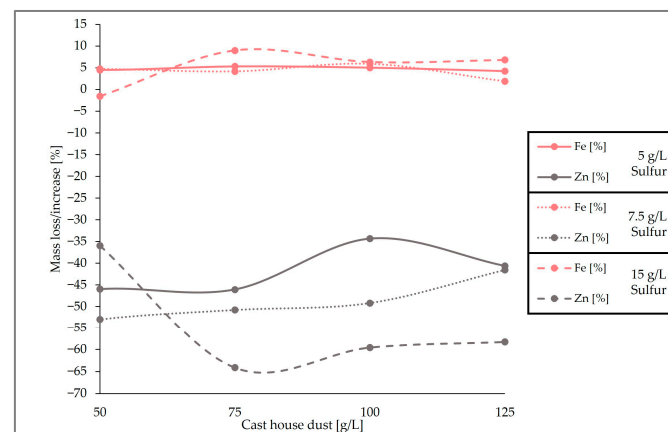


Figure 12. Comparison of the removal efficiency of Fe and Zn for different cast house dust concentrations and 5, 7.5, and 15 g/L of sulfur.

Despite residual amounts of sulfur in the leached dust being undesired for further recirculation in the steel mill, sufficient sulfur (either in the solid sample or as elemental sulfur) must be available for the microorganisms to catalyze the bioleaching of zinc. Additionally, higher dust concentrations are preferred to increase the amount of dust treated per batch. For this reason, the remaining sulfur in the leached dust was calculated as a function of the concentration of the cast house dust to determine the maximum allowable dust concentration that can be added for a determined added sulfur concentration.

Due to the promising results afforded by sulfur concentrations of 15 g/L, and considering that one of the premises for the recirculation of the treated dust is the absence of additional sulfur, the remaining sulfur content in the leached cast house dust was analyzed for run3 (15 g/L S). The change in mass content of elemental sulfur present in the solid residue with increasing cast house dust concentrations was calculated according to Equation (3) for run3, as displayed in Figure 13. This shows the total consumption of the added sulfur for dust concentrations of 125 g/L.

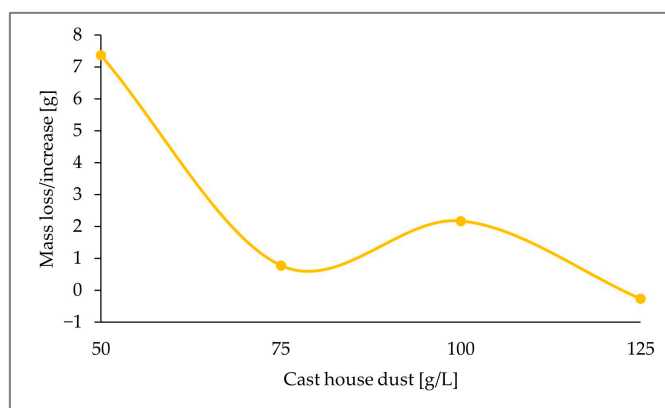


Figure 13. Sulfur weight variation with increasing cast house dust concentration and 15 g/L of sulfur (run3).

Additional X-ray diffraction (XRD) analyses were carried out to confirm the absence of sulfur and to check the evolution of the mineralogical composition of the leached dust through the experiments. For this purpose, the untreated cast house dust, as well as the leached dust after the consecution of the experiments with a sulfur content of 15 g/L and a dust concentration of 125 g/L, were analyzed. Therefore, one sample of the dust suspended in the leachate (run3, 125 g/L dust) was collected, filtered, dried, and analyzed. The results of the analyses are shown in Figure 14. Looking at the final composition and comparing it with the initial substrate's structure, the absence of sulfur or zinc compounds in the final leached substrate, together with an enrichment of hematite (Fe^{3+}), can be observed, which might confirm the *A. ferrooxidans* oxidation mechanism from Fe^{2+} to Fe^{3+} , since this bacterium is known to be capable of oxidizing both iron and sulfur, as confirmed by previous studies [20].

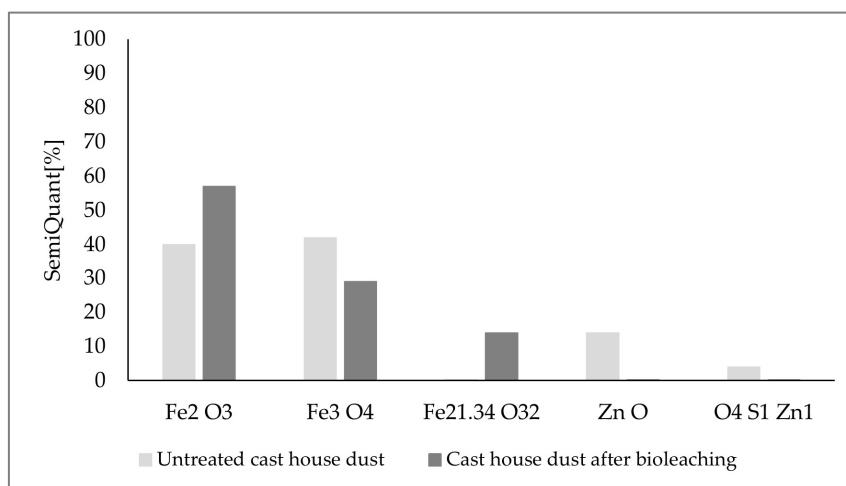


Figure 14. XRD analyses results for the untreated cast house dust and cast house dust after bioleaching using 15 g/L sulfur and 125 g/L of dust concentrations.

5. Conclusions

The best results in direct bioleaching of cast house dust with different sulfur concentrations were obtained with the addition of 15 g/L sulfur, where the highest zinc removal efficiency (between 60% (*w/w*) and 70% (*w/w*)) and, therefore, the highest enrichment of iron in the solid were achieved. Additionally, the consumption of elemental sulfur by *A. ferrooxidans* and *A. thiooxidans*, as well as a decreased leaching of iron with lower sulfur concentrations, was confirmed. The study of the behavior of the system with higher cast

house dust concentrations, with longer periods of time, as well as the upscale of the system to 100 or 1000 L would be interesting for further analysis.

Author Contributions: Conceptualization, A.S., M.H. and S.T.; methodology, A.S., M.H. and S.T.; formal analysis, A.S.; investigation, A.S. and C.H.; resources, L.B.; data curation, A.S.; writing—original draft preparation, A.S.; writing—review and editing, M.H., S.T., S.S., C.H., L.B. and M.W.; visualization, A.S.; supervision, M.H. and L.B.; project administration, M.H.; funding acquisition, M.H. All authors have read and agreed to the published version of the manuscript.

Funding: The authors gratefully acknowledge the funding support of K1-MET GmbH, Metallurgical Competence Center. K1-MET GmbH is a COMET Centre within the COMET—Competence Centers for Excellent Technologies Program and funded by the Federal Ministry for Climate Action, Environment, Energy, Mobility, Innovation and Technology; the Federal Ministry for Labor and Economy; the provinces Upper Austria, Styria and Tyrol. Apart from funding, the project activities are financed by the industrial partner voestalpine Stahl GmbH.

Data Availability Statement: Not applicable.

Acknowledgments: The authors would like to express their gratitude to voestalpine Stahl GmbH, for the for the fruitful discussions and cooperation.

Conflicts of Interest: The authors declare no conflict of interest.

References

1. Rieger, J.; Colla, V.; Matino, I.; Branca, T.A.; Stubbe, G.; Panizza, A.; Brondi, C.; Falsafi, M.; Hage, J.; Wang, X.; et al. Residue Valorization in the Iron and Steel Industries: Sustainable Solutions for a Cleaner and More Competitive Future Europe. *Metals* **2021**, *11*, 1202. [[CrossRef](#)]
2. Xue, Y.; Hao, X.; Liu, X.; Zhang, N. Recovery of Zinc and Iron from Steel Mill Dust—An Overview of Available Technologies. *Materials* **2022**, *15*, 4127. [[CrossRef](#)] [[PubMed](#)]
3. Singh, L.; Ranjan, M. *Dezincification from Blast Furnace Sludge/Dust*; Department of Metallurgy and Materials Science: Pune, India, 2018.
4. Lanzertstorfer, C. Dust recycling in integrated steel mills: Reducing of zinc recirculation. In Proceedings of the METAL 2022, Brno, Czech Republic, 18–19 May 2022.
5. Gomes, H.; Funari, V.; Mayes, W.M.; Rogerson, M.; Prior, T.J. Recovery of Al, Cr and V from steel slag by bioleaching: Batch and column experiments. *J. Environ. Manag.* **2018**, *222*, 30–36. [[CrossRef](#)] [[PubMed](#)]
6. Vestola, E.A.; Kuusenaho, M.K.; Närhi, H.M.; Tuovinen, O.H.; Puhakka, J.A.; Plumb, J.J.; Kaksonen, A. Acid bioleaching of solid waste materials from copper, steel and recycling industries. *Hydrometallurgy* **2010**, *103*, 74–79. [[CrossRef](#)]
7. Hocheng, H.; Su, C.; Jadhav, U.U. Bioleaching of metals from steel slag by *Acidithiobacillus thiooxidans* culture supernatant. *Chemosphere* **2014**, *117*, 652–657. [[CrossRef](#)] [[PubMed](#)]
8. Srichandan, H.; Mohapatra, R.K.; Parhi, P.K.; Mishra, S. Bioleaching approach for extraction of metal values from secondary solid wastes: A critical review. *Hydrometallurgy* **2019**, *189*, 105122. [[CrossRef](#)]
9. Andersson, A. Recycling of Blast Furnace Sludge within the Integrated Steel Plant: Potential for Complete Recycling and Influence on Operation. Ph.D. Thesis, Luleå University of Technology, Luleå, Sweden, 2019.
10. Babich, A.; Senk, D.; Gudenau, H.W.; Mavrommatis, K. *Ironmaking*; RWTH Aachen University, Department of Ferrous Metallurgy: Aachen, Germany, 2008.
11. Lanzerstorfer, C. Characterization of dust from blast furnace cast house de-dusting. *Environ. Technol.* **2016**, *38*, 2440–2446. [[CrossRef](#)] [[PubMed](#)]
12. Lanzerstorfer, C.; Angerbauer, A.; Gaßlbauer, M. Feasibility of Air Classification in Dust Recycling in the Iron and Steel Industry. *Steel Res. Int.* **2018**, *89*, 1800017. [[CrossRef](#)]
13. Bayat, O.; Sever, E.; Bayat, B.; Arslan, V.; Poole, C. Bioleaching of Zinc and Iron from Steel Plant Waste using *Acidithiobacillus ferrooxidans*. *Appl. Biochem. Biotechnol.* **2009**, *152*, 117–126. [[CrossRef](#)] [[PubMed](#)]
14. Park, P.; Liang, Y. Bioleaching of trace elements and rare earth elements from coal fly ash. *Int. J. Coal Sci. Technol.* **2019**, *6*, 74–83. [[CrossRef](#)]
15. Kremser, K.; Thallner, S.; Strbik, D.; Spiess, S.; Kucera, J.; Vaculovic, T.; Vsiansky, D.; Haberbauer, M.; Mandl, M.; Guebitz, G.M. Leachability of metals from waste incineration residues by iron- and sulfur-oxidizing bacteria. *J. Environ. Manag.* **2021**, *280*, 111734. [[CrossRef](#)]
16. Bosecker, K. Bioleaching: Metal solubilization by microorganisms. *FEMS Microbiol. Rev.* **1997**, *20*, 591–604. [[CrossRef](#)]
17. Monachon, M.; Albelda-Berenguer, M.; Joseph, E. Biological oxidation of iron sulfides. *Adv. Appl. Microbiol.* **2019**, *107*, 1–27. [[CrossRef](#)] [[PubMed](#)]
18. Yang, L.; Zhao, D.; Yang, J.; Wang, W.; Chen, P.; Zhang, S.; Yan, L. *Acidithiobacillus thiooxidans* and its potential application. *Appl. Microbiol. Biotechnol.* **2019**, *103*, 7819–7833. [[CrossRef](#)] [[PubMed](#)]

19. Kremser, K.; Thallner, S.; Schoen, H.; Weiss, S.; Hemmelmaier, C.; Schnitzhofer, W.; Aldrian, A.; Guebitz, G.M. Stirred-tank and heap-bioleaching of shredder-light-fractions (SLF) by acidophilic bacteria. *Hydrometallurgy* **2020**, *193*, 105315. [[CrossRef](#)]
20. Bayat, B.; Sari, B. Comparative evaluation of microbial and chemical leaching processes for heavy metal removal from dewatered metal plating sludge. *J. Hazard. Mater.* **2010**, *174*, 763–769. [[CrossRef](#)] [[PubMed](#)]
21. Wakeman, K.; Auvinen, H.; Johnson, D.B. Microbiological and Geochemical Dynamics in Simulated-Heap Leaching of a Polymetallic Sulfide Ore. *Biotechnol. Bioeng.* **2008**, *101*, 739–750. [[CrossRef](#)] [[PubMed](#)]
22. Miranda-Arroyave, L.M.; Márquez-Godoy, M.A.; Ocampo-Carmona, L.M. Adaptation of *Acidithiobacillus ferrooxidans*, *Acidithiobacillus thiooxidans* and *Leptospirillum ferrooxidans* strains on sphalerite concentrate from mining waste. *Respuestas* **2019**, *24*, 72–83. [[CrossRef](#)]
23. Wu, X.; Zhang, Z.; Liu, L.; Deng, F.; Liu, X.; Qiu, G. Metal Resistance-Related Genes are Differently Expressed in Response to Copper and Zinc Ion in Six *Acidithiobacillus ferrooxidans* Strains. *Curr. Microbiol.* **2014**, *69*, 775–784. [[CrossRef](#)] [[PubMed](#)]
24. Kondratyeva, T.F.; Muntyan, L.N.; Karavaiko, G.I. Zinc- and arsenic-resistant strains of *Thiobacillus ferrooxidans* have increased copy numbers of chromosomal resistance genes. *Microbiology* **1995**, *141*, 1157–1162. [[CrossRef](#)]

Disclaimer/Publisher’s Note: The statements, opinions and data contained in all publications are solely those of the individual author(s) and contributor(s) and not of MDPI and/or the editor(s). MDPI and/or the editor(s) disclaim responsibility for any injury to people or property resulting from any ideas, methods, instructions or products referred to in the content.